Ventral hippocampus interacts with prelimbic cortex during inhibition of threat response via learned safety in both mice and humans

Heidi C. Meyer[a,1], Paola Odriozola[b,1], Emily M. Cohodes[b], Jeffrey D. Mandell[c], Anfei Li[a], Ruirong Yang[a], Baila S. Hall[d], Jason T. Haberman[b], Sadie J. Zacharek[b], Conor Liston[e,f], Francis S. Lee[a,e,2,3], and Dylan G. Gee[b,2,3]

[a]Department of Psychiatry, Weill Cornell Medicine, New York, NY 10065; [b]Department of Psychology, Yale University, New Haven, CT 06511; [c]Program in Computational Biology and Bioinformatics, Yale University, New Haven, CT 06511; [d]Department of Psychology, Brain Research Institute, University of California, Los Angeles, CA 90095; [e]Sackler Institute for Developmental Psychobiology, Weill Cornell Medicine, New York, NY 10065; and [f]Feil Family Brain & Mind Research Institute, Weill Cornell Medicine, New York, NY 10065

Edited by Bruce S. McEwen, Rockefeller University, New York, NY, and approved November 8, 2019 (received for review June 25, 2019)

Heightened fear and inefficient safety learning are key features of fear and anxiety disorders. Evidence-based interventions for anxiety disorders, such as cognitive behavioral therapy, primarily rely on mechanisms of fear extinction. However, up to 50% of clinically anxious individuals do not respond to current evidence-based treatment, suggesting a critical need for new interventions based on alternative neurobiological pathways. Using parallel human and rodent conditioned inhibition paradigms alongside brain imaging methodologies, we investigated neural activity patterns in the ventral hippocampus in response to stimuli predictive of threat or safety and compound cues to test inhibition via safety in the presence of threat. Distinct hippocampal responses to threat, safety, and compound cues suggest that the ventral hippocampus is involved in conditioned inhibition in both mice and humans. Moreover, unique response patterns within target-differentiated subpopulations of ventral hippocampal neurons identify a circuit by which fear may be inhibited via safety. Specifically, ventral hippocampal neurons projecting to the prelimbic cortex, but not to the infralimbic cortex or basolateral amygdala, were more active to safety and compound cues than threat cues, and activity correlated with freezing behavior in rodents. A corresponding distinction was observed in humans: hippocampal–dorsal anterior cingulate cortex functional connectivity—but not hippocampal–anterior ventromedial prefrontal cortex or hippocampal–basolateral amygdala connectivity—differentiated between threat, safety, and compound conditions. These findings highlight the potential to enhance treatment for anxiety disorders by targeting an alternative neural mechanism through safety signal learning.

safety learning | threat | conditioned inhibition | hippocampus | anxiety

Although fear can contribute to survival by increasing vigilance and facilitating the avoidance of potential danger, difficulty regulating threat responses is the hallmark of stress-related and anxiety disorders (1). These disorders are the most common psychiatric illnesses, affecting up to one-third of the population (2) and amounting to over 260 million individuals worldwide (3). Although evidence-based treatments for anxiety disorders exist, they have limited long-term efficacy for up to 50% of patients (4, 5), highlighting the need to optimize current treatments based on the neurobiology of fear reduction.

Decades of cross-species research have investigated the intricacies of threat learning (6, 7), but less is known about the mechanisms by which fear can be regulated, particularly when a fear-provoking stimulus may also be present. Moreover, the majority of studies on mechanisms underlying fear reduction have focused on extinction learning. This form of learning is subject to the relapse of fear, in part because the same stimulus is conferred with competing threat and safety representations (8). Furthermore, extinction learning has been shown to be weaker in individuals with anxiety (9, 10), who also show weaker connectivity between frontoamygdala regions (11) that are critical for mediating fear expression and extinction across species (12, 13). The primary evidence-based behavioral treatment for individuals with anxiety, cognitive behavioral therapy (CBT), is based on principles of fear extinction and is thought to rely on frontoamygdala circuitry (14), suggesting the potential to optimize treatment via mechanisms of fear reduction that target alternative pathways. Safety signal learning, in contrast to extinction, involves the ability to associate distinct environmental stimuli (i.e., safety signals) with the nonoccurrence of aversive events (15). Following repeated presentations, a stimulus predicting the explicit absence of an aversive outcome can develop "safe" properties capable of modulating, or inhibiting, threat responding through a process referred to as conditioned inhibition (15, 16). Safety signals have been shown to be effective for reducing threat responding and preventing the onset of new fears in rodents (16), nonhuman primates (17), and healthy adult humans (18); however, much remains unknown about their neural bases.

Significance

Although fear can contribute to survival, difficulty regulating threat responses can interfere with goal-directed activities and is the hallmark of anxiety disorders. These disorders are the most common psychiatric illnesses, affecting up to one-third of the population. In parallel studies across species, we identify a pathway that engages the ventral hippocampus for the attenuation of threat responses through conditioned inhibition. Conditioned inhibition relies on the specific involvement of ventral hippocampal neurons projecting to the prelimbic cortex in mice and homologous ventral hippocampal–dorsal anterior cingulate cortex functional connectivity in humans. These findings highlight a pathway for the inhibition of fear with the potential to enhance interventions for anxiety disorders by targeting an alternative neural circuitry through safety signal learning.

Author contributions: H.C.M., P.O., E.M.C., J.T.H., F.S.L., and D.G.G. designed research; H.C.M., P.O., E.M.C., R.Y., J.T.H., and S.J.Z. performed research; P.O., J.D.M., B.S.H., S.J.Z., and C.L. contributed new reagents/analytic tools; H.C.M., P.O., A.L., B.S.H., S.J.Z., C.L., and D.G.G. analyzed data; and H.C.M., P.O., E.M.C., F.S.L., and D.G.G. wrote the paper.

The authors declare no competing interest.

This article is a PNAS Direct Submission.

Data deposition: Data used for these studies have been deposited in the Open Science Framework Repository (https://osf.io/nqryd/).

[1]H.C.M. and P.O. contributed equally to this work.

[2]F.S.L. and D.G.G. contributed equally to this work.

[3]To whom correspondence may be addressed. Email: fslee@med.cornell.edu or dylan.gee@yale.edu.

This article contains supporting information online at https://www.pnas.org/lookup/suppl/doi:10.1073/pnas.1910481116/-/DCSupplemental.

First published December 10, 2019.

Despite advances in identifying the neural correlates of a safety signal and the process by which an individual discriminates between threat and safety cues (19–31), little is known about the mechanisms by which a safety signal actively attenuates threat responding (i.e., conditioned inhibition). A region of potential interest in this regard is the ventral hippocampus. The rodent ventral hippocampus, which may correspond to the anterior portion of the human hippocampus (hereafter referred to as ventral hippocampus), has been implicated in emotion and threat learning (32, 33) and encoding anxiogenic environments (34). Emerging evidence suggests ventral hippocampus gates threat responding predominantly under conditions of associative competition (35), such as responding to an extinguished threat cue that occurs outside of the extinction context (36, 37). The ventral hippocampus has been shown in rodents to be integral for the acquisition and expression of conditioned fear (38, 39), though not the acquisition of safety signals (40). However, under specific circumstances the hippocampus has been linked to the retrieval of learned safety and subsequent modulation of a threat response (41, 42). Notably, how the ventral hippocampus is engaged during the conditioned inhibition of threat responding via safety signals has yet to be established.

In the present study, we investigated the neural substrates of conditioned inhibition using a translational approach to explore the circuit-based mechanism by which safety signals gate the expression of threat responding in both mice and humans. In mice, fiber photometry recordings were utilized to examine neural ensemble activity in the ventral hippocampus during a conditioned inhibition task. Recording neural activity during a summation test in addition to discrete threat and safety cues allowed us to examine circuit activity during the active inhibition of threat responding, thus providing insight into the neural mechanisms underlying conditioned inhibition. In humans, functional MRI (fMRI) data from healthy adults ages 18 to 30 were collected to examine ventral hippocampal activation during a conditioned inhibition task, constituting a neural mechanistic examination of conditioned inhibition in the face of threat in humans.

In order to isolate circuit-specific activity emerging in response to threat and safety cues as well as the conditioned inhibition of threat responding, we systematically elucidated the role of specific neuronal populations within the ventral hippocampus projecting to prelimbic cortex (PL), infralimbic cortex (IL), or basolateral amygdala (BLA) in the implementation of safety behavior in mice. In parallel, in humans, we examined task-related functional connectivity between the ventral hippocampus and the dorsal anterior cingulate (dACC) and anterior ventromedial prefrontal cortex (vmPFC), correlates of the rodent PL and IL, respectively (14, 43, 44), as well as the BLA, to elucidate the involvement of specific hippocampal circuitry in conditioned inhibition.

Results

Behavioral Results in Mice. Mice were trained to discriminate between a threat cue (a tone paired with a mild footshock) and a safety cue (a distinct tone, unpaired) (Fig. 1 *A*, *Top*). During the testing phase, mice were separated into 3 groups and exposed to 1 of the following conditions: threat, safety, or a simultaneous "compound" presentation of both cues (i.e., summation) (Fig. 1 *A*, *Bottom*). Consistent with hypotheses, freezing behavior differed between the 3 conditions (Fig. 1*C*). In mice expressing the calcium-binding fluorescent reporter virus (GCaMP) in cumulative ventral hippocampal neurons, a 1-way ANOVA revealed a significant effect of condition on freezing, $F(2, 35) = 18.90$, $P < 0.001$, $\eta^2 = 0.52$. A significant linear contrast confirmed that overall freezing behavior was highest during presentations of the threat cue, lower during the compound cue, and lowest during the safety cue, $F(1, 35) = 37.54$, $P < 0.001$, $\eta^2 = 0.52$. This linear decrease in freezing behavior in response to the 3 conditions (i.e., threat > compound > safety) was replicated in independent surgical groups of mice expressing a Cre-dependent strain of the GCaMP virus (GCaMP-FLEX) in ventral hippocampal neurons along with Cre recombinase in PL (*SI Appendix*, Fig. S3, $F(1, 39) = 149.32$, $P < 0.001$, $\eta^2 = 0.75$), IL (*SI Appendix*, Fig. S5*B*,

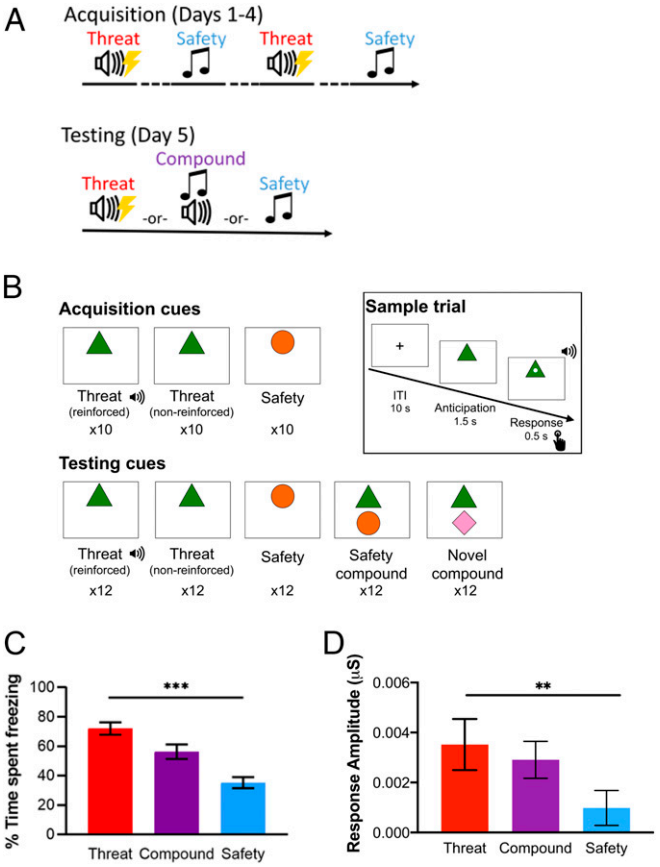

Fig. 1. Cross-species experimental designs, and behavioral and physiological responses. (*A*) Conditioned inhibition task design in mice. The acquisition phase of the task took place over 4 consecutive days. Each day included 2 trials of a threat cue (20 s) reinforced by a coterminating US (mild footshock, 0.5 mA, 1-s duration) and 30 trials of a nonreinforced safety cue (20 s). Trials occurred on a variable intertrial interval (ITI; 30 to 90 s) schedule, and trial order was varied daily. On the testing day, mice were separated into 3 groups (1 group per condition) and presented with 10 trials (each 20 s) of one of the following cues: nonreinforced threat, nonreinforced safety, and threat–safety compound. Trials occurred on a 60-s ITI schedule. Cues were 2.9-kHz and 12.5-kHz tones, counterbalanced into each condition. (*B*) Conditioned inhibition task design in humans. The acquisition phase of the task included 10 trials of a threat cue, which was reinforced by the US (an aversive sound), 10 trials of a nonreinforced threat cue, and 10 trials of a safety cue that was never reinforced. The testing phase included 12 trials of each of the following cues: reinforced threat, nonreinforced threat, safety, safety compound (i.e., paired threat and safety cues), and novel compound (i.e., paired threat and novel cues). The sample trial shows the timing of the task, in which an ITI (fixation cross) was presented for 10 s, followed by an anticipation period in which the cue was presented for 1.5 s, and followed by a response period lasting 0.5 s in which a white dot appeared at the center of the shape and participants were instructed to make a button press. The US onset coterminated with the response period on reinforced trials only. (*C*) Task-related behavioral responses in mice. Mean percentage of time spent freezing by task condition in the testing phase revealed a linear effect in which freezing to threat cue was highest and safety cue was lowest, $P < 0.001$, $\eta^2 = 0.52$. Threat condition: $n = 13$; compound condition: $n = 12$; safety condition: $n = 13$. (*D*) Task-related physiological responses in humans. Mean skin conductance response (SCR) by task condition in testing phase revealed a linear effect in which SCR to threat cue was highest and safety cue was lowest, $n = 22$, $P = 0.004$, $\eta_p^2 = 0.38$. All error bars show ± 1 SEM. $^{**}P < 0.01$, $^{***}P < 0.001$.

$F(1, 33) = 59.36$, $P < 0.001$, $\eta^2 = 0.63$), or BLA (*SI Appendix*, Fig. S8*B*, $F(1, 27) = 91.43$, $P < 0.001$, $\eta^2 = 0.70$), confirming that mice successfully learned to discriminate between threat and safety cues, and also acquired a safety signal capable of conditioned inhibition.

Physiological Results in Humans. In order to test the efficacy of safety signals to reduce fear-related reactivity, skin conductance response (SCR) was measured as an index of physiological reactivity during the conditioned inhibition task in humans (Fig. 1*B*). A repeated-measures ANCOVA revealed a significant effect of condition on SCR, $F(2,36) = 3.99$, $P = 0.027$, $\eta_p^2 = 0.18$. Consistent with hypotheses, a significant linear contrast confirmed that mean SCR was highest to the threat cue, lower in response to the pairing of threat and safety cues (i.e., compound condition), and lowest to the safety cue, $F(1,18) = 10.84$, $P = 0.004$, $\eta_p^2 = 0.38$ (Fig. 1*D*).

Ventral Hippocampal Activity in Mice. Four weeks prior to behavioral training, mice were infused with a calcium-binding fluorescent

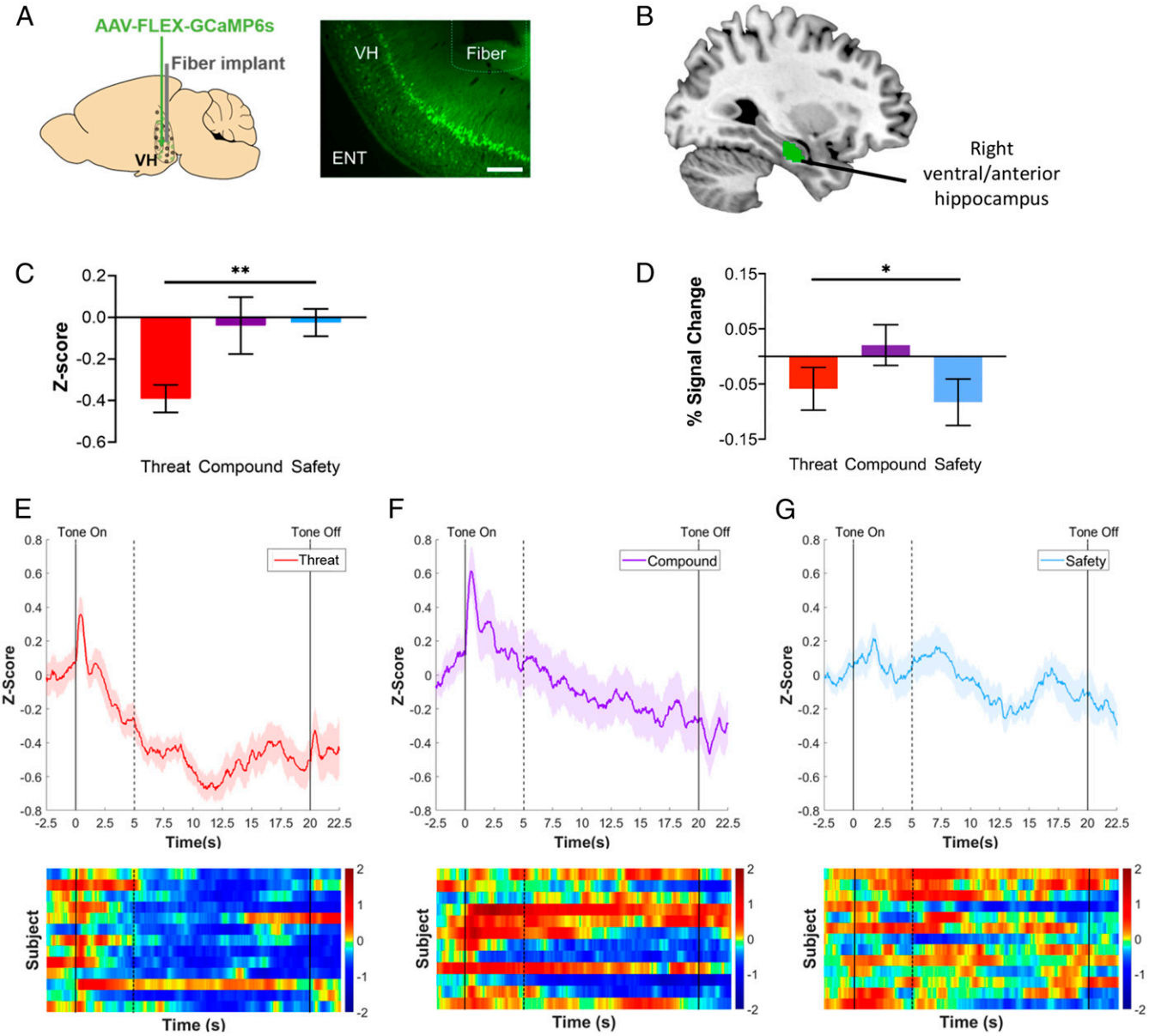

Fig. 2. Cross-species ventral hippocampal responses. (*A*) Schematic of fiber photometry targeted to ventral hippocampus in mice. (*Left*) Schematic of injection site for AAV-FLEX-GCaMP6s and fiber placement (ventral hippocampus). (*Right*) Representative example of GCaMP expression and fiber placement in ventral hippocampal cell bodies. (10× magnification, scale bar, 200 μm.) ENT, entorhinal cortex; VH, ventral hippocampus. (*B*) Ventral hippocampus ROI in humans. The right ventral/anterior hippocampus ROI examined in the present study (green) was obtained from ref. 66. (*C*) Neural activity by condition in mice. Mean z-score of calcium signal recorded from ventral hippocampal neurons showed a significant linear contrast in which neural activity was highest during the threat cue and lowest during the safety cue, $P = 0.008$, $\eta^2 = 0.18$. Threat condition: $n = 13$; compound condition: $n = 12$; safety condition: $n = 13$. (*D*) Task-related ventral hippocampal response in humans. Mean percent signal change extracted from the right ventral hippocampus ROI showed a significant quadratic contrast indicating that activation in the right ventral hippocampus was higher during the compound cue relative to both the threat cue and the safety cue, $n = 50$, $P = 0.020$, $\eta_p^2 = 0.11$. (*E*–*G*) Fiber photometry traces recorded from cumulative ventral hippocampus. Traces of z-scored calcium signal and corresponding heatmaps for the threat condition (*E*), compound condition (*F*), and safety condition (*G*). Solid lines indicate tone onset (0 s) and offset (20 s). Dashed line indicates tone onset-induced activity for corresponding timeseries data. All error bars show ± 1 SEM. $^*P < 0.05$, $^{**}P < 0.01$.

reporter (AAV-hSyn-GCaMP6s) and implanted with a fiber-optic cannula into the ventral hippocampus (Fig. 2*A*). During the testing phase, activity patterns in GCaMP-expressing neurons in the ventral hippocampus were recorded using the in vivo calcium imaging technique, fiber photometry (45) (Fig. 2 *C* and *E*–*G*). Overall, ventral hippocampal activity was lowest during presentations of the threat cue (1-way ANOVA, $F(2, 35) = 5.09$, $P = 0.012$, $\eta^2 = 0.23$), with a linear increase in activity apparent across threat, compound, and safety cues (linear contrast, $F(1, 35) = 8.02$, $P = 0.008$, $\eta^2 = 0.18$), suggesting the ventral hippocampus may play a role in regulating threat responding. A linear regression across all 3 groups showed that average neural activity was not associated with freezing behavior, $F(1, 36) = 1.80$, $P = 0.189$, $\eta^2 = 0.05$ (*SI Appendix*, Fig. S1), suggesting that, cumulatively, the ventral hippocampus is involved in processing the safety information of a cue, though not directly influencing overt threat behavior.

Ventral Hippocampal Activity in Humans. fMRI data were collected during the conditioned inhibition task in humans to assess the involvement of the ventral hippocampus across conditions of threat, safety, and conditioned inhibition using the pairing of threat and safety cues (i.e., compound condition). A repeated-measures ANCOVA revealed a significant quadratic contrast indicating that activation in the right ventral hippocampus (Fig. 2*B*) was higher during the compound cue relative to both the threat cue and the safety cue alone, $F(1,46) = 5.80$, $P = 0.020$, $\eta_p^2 = 0.11$, suggesting involvement of the ventral hippocampus in conditioned inhibition (Fig. 2*D*). There was also a trend-level within-subjects effect of condition for activation in the right ventral hippocampus, $F(2,92) = 2.96$, $P = 0.057$, $\eta_p^2 = 0.06$. There was no effect of condition for activation in the left ventral hippocampus, $F(2,92) = 0.57$, $P = 0.565$, $\eta_p^2 = 0.01$.

Ventral Hippocampal Neurons Inhibit Threat Responding via Safety in a Target-Defined Manner in Mice. To examine the role of ventral hippocampal connectivity in conditioned inhibition, mice were infused with a Cre-dependent strain of the calcium-binding fluorescent reporter (AAV-hSyn-FLEX-GCaMP6s) into the ventral hippocampus, and retrograde Cre recombinase (rAAV2-retro Cre) into the PL (Fig. 3*A*) in order to selectively express GCaMP in ventral hippocampal neurons projecting to the PL. In addition, a fiber-optic cannula was implanted into the ventral hippocampus. During the testing phase, neural activity in the PL-projecting ventral hippocampal neurons (Fig. 3 *C* and *E*–*G*) was lowest during presentations of the threat cue (1-way ANOVA, $F(2, 39) = 8.29$, $P = 0.001$, $\eta^2 = 0.30$), with a linear increase in overall activity during the compound and safety cues (linear contrast, $F(1, 39) = 15.93$, $P < 0.001$, $\eta^2 = 0.29$). In addition, a linear regression across all 3 groups revealed a negative correlation between average freezing behavior and average neural activity, such that mice with the highest signaling in PL-projecting ventral hippocampal neurons also exhibited the lowest freezing behavior (Fig. 3*H*), $F(1, 40) = 2.98$, $P = 0.002$, $\eta^2 = 0.21$, suggesting that the modulation of an overt threat response is related to the level of activity in this subpopulation of neurons.

Two additional groups of mice received infusions of the Cre-dependent fluorescent reporter (AAV-hSyn-FLEX-GCaMP6s) into the ventral hippocampus and Cre recombinase (rAAV2-retro Cre) into the IL (*SI Appendix*, Fig. S5*A*) or BLA (*SI Appendix*, Fig. S8*A*) and were implanted with a fiber-optic cannula into the ventral hippocampus. In contrast to PL-projecting ventral hippocampal neurons, average neural activity in IL-projecting neurons (*SI Appendix*, Fig. S5*F*) did not significantly differ between groups, with only a marginal trend apparent, $F(2, 33) = 2.63$, $P = 0.087$, $\eta^2 = 0.14$. In addition, a linear regression across all 3 groups showed that average neural activity did not predict freezing behavior (*SI Appendix*, Fig. S5*G*), $F(1, 34) = 2.50$, $P = 0.120$, $\eta^2 = 0.07$. Likewise, average neural activity in BLA-projecting neurons did not differ by condition, $F(2, 27) = 0.53$, $P = 0.595$, $\eta^2 = 0.04$, nor did it correlate with freezing behavior, $F(1, 28) = 0.72$, $P = 0.403$, $\eta^2 = 0.03$ (*SI Appendix*, Fig. S8 *F* and *G*).

Ventral Hippocampal Functional Connectivity with dACC but Not Anterior vmPFC or BLA Responds to Threat Inhibition in Humans. In humans, a generalized psychophysiological interaction (gPPI) analysis was conducted to examine ventral hippocampal functional connectivity during conditioned inhibition. Specifically, we compared ventral hippocampal functional connectivity with the dACC, with the anterior vmPFC, and with the BLA using separate repeated-measures ANCOVAs for each region of interest (ROI)'s connectivity with the right and left ventral hippocampus ROI. A significant effect of condition was observed for left ventral hippocampus–dACC functional connectivity, $F(2,88) = 3.43$, $P = 0.037$, $\eta_p^2 = 0.07$. The linear contrast of condition was significant such that functional connectivity was higher in the compound and safety conditions, relative to the threat condition, $F(1,44) = 5.47$, $P = 0.024$, $\eta_p^2 = 0.11$, suggesting differential functional connectivity between the ventral hippocampus and dACC in the presence of a safety signal (Fig. 3*D*). Furthermore, there were no significant effects for left ventral hippocampal–anterior vmPFC functional connectivity, $F(2,88) = 0.25$, $P = 0.782$, $\eta_p^2 = 0.01$ (*SI Appendix*, Fig. S7), or left ventral hippocampal–BLA functional connectivity, $F(2,88) = 0.32$, $P = 0.728$, $\eta_p^2 = 0.01$ (*SI Appendix*, Fig. S10), suggesting the specificity of hippocampal–dACC functional connectivity in conditioned inhibition. There were no significant effects for right ventral hippocampal–dACC functional connectivity, $F(2,88) = 0.25$, $P = 0.782$, $\eta_p^2 = 0.01$, right ventral hippocampal–anterior vmPFC functional connectivity, $F(2,88) = 1.61$, $P = 0.205$, $\eta_p^2 = 0.04$, or right ventral hippocampal–BLA functional connectivity, $F(2,88) = 0.67$, $P = 0.512$, $\eta_p^2 = 0.02$.

Temporal Dynamics of Ventral Hippocampal Activity Differs by Condition in Mice. Changes in neural activity throughout the duration of a cue (i.e., the temporal dynamics of neural activity) provide insight into neural circuit engagement during threat and safety cues, as well as the inhibition of threat responding. Patterns of neural activity induced by the onset of a cue are of particular interest as a measure of the initial processing of the cue's meaning. Thus, we analyzed the temporal distribution of peak calcium signal (top 5% of tone-induced signal) as a measure of variability in neural responding throughout the duration of each cue. The proportion of signal occurring during 4 discrete time epochs during each 20-s cue (0 to 5 s, 6 to 10 s, 11 to 15 s, and 16 to 20 s; Fig. 3 *I* and *J*) was calculated based on the cumulative frequency distribution of the proportion of peak calcium signal across the 20-s tone. The initial 5-s epoch served as a comparison point for all subsequent epochs.

A 2-way repeated measures ANOVA revealed a main effect of epoch, $F(3, 117) = 13.11$, $P < 0.001$, $\eta_p^2 = 0.23$, a main effect of condition, $F(2, 39) = 6.97$, $P = 0.003$, $\eta_p^2 < 0.001$, and an interaction between epoch and condition, $F(6, 117) = 3.33$, $P = 0.005$, $\eta_p^2 = 0.12$, indicating that the timeseries for peak calcium signal differed between threat, safety, and compound cues. Follow-up analyses to deconstruct the interaction compared the proportion of peak calcium signal induced by tone onset (0 to 5 s) to the proportion of peak calcium signal recorded in the 3 subsequent time epochs: 6 to 10 s, 11 to 15 s, and 16 to 20 s. A Tukey honest significant difference (HSD) test indicated that threat cues, but not safety or compound cues, were associated with a greater proportion of peak calcium signal occurring at tone onset (0 to 5 s) relative to all other epochs (6 to 10 s, $P = 0.005$; 11 to 15 s, $P = 0.030$; 16 to 20 s, $P = 0.013$). This transient coordination of neuronal firing elicited by the threat cue may reflect initial processing of the presence of a threat. A slight elevation at tone onset was apparent during compound cues, although only relative to signal following tone midpoint (11 to 15 s, $P = 0.009$). Peak calcium signal across

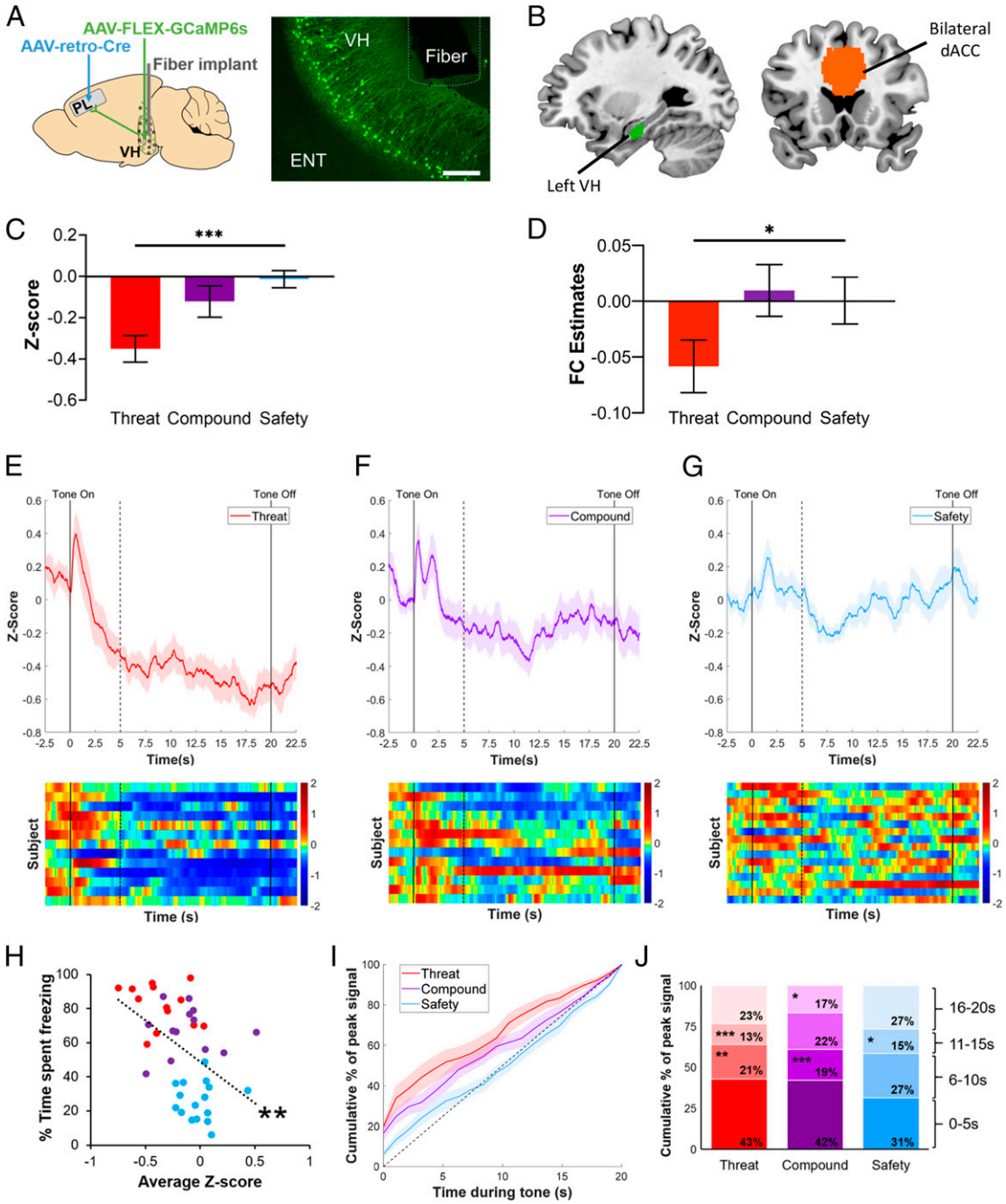

Fig. 3. Ventral hippocampus to prelimbic cortex projection in mice and humans. (*A*) Schematic of fiber photometry targeted to prelimbic-projecting ventral hippocampal neurons in mice. (*Left*) Schematic of injection site for AAV-FLEX-GCaMP6s (ventral hippocampus), injection site for retro-Cre (prelimbic cortex), and fiber placement (ventral hippocampus). (*Right*) Representative example of GCaMP expression and fiber placement in ventral hippocampal cell bodies (10× magnification, scale bar, 200 μm). ENT, entorhinal cortex; PL, prelimbic cortex; VH, ventral hippocampus. (*B*) Left ventral hippocampus and dACC ROIs in humans. The left ventral/anterior hippocampus ROI (green) examined in the present study was obtained from ref. 66. The bilateral dACC ROI (orange) was defined as in ref. 68. A generalized psychophysiological interaction was implemented in FSL to extract estimates of functional connectivity between these 2 regions. (*C*) Neural activity by condition in mice. Mean z-score of calcium signal recorded from prelimbic-projecting ventral hippocampal neurons showed a significant linear contrast in which neural activity was highest during the threat cue and lowest during the safety cue, $P < 0.001$, $\eta^2 = 0.29$. Threat condition: $n = 13$; compound condition: $n = 13$; safety condition: $n = 16$. (*D*) Left ventral hippocampus to dACC functional connectivity. A significant linear contrast of condition showed that functional connectivity was lowest for the threat condition and highest for the safety and compound conditions, $n = 48$, $P = 0.024$, $\eta_p^2 = 0.11$. (*E*–*G*) Fiber photometry traces recorded from prelimbic-projecting ventral hippocampal neurons. Trace of z-scored calcium signal and corresponding heatmaps for the threat condition (*E*), compound condition (*F*), and safety condition (*G*). Solid lines indicate tone onset (0 s) and offset (20 s). Dashed line indicates tone onset-induced activity for corresponding timeseries data. (*H*) Relationship between neural activity and freezing behavior. A linear regression revealed a negative correlation between neural activity and average freezing behavior in prelimbic-projecting ventral hippocampal neurons, such that mice with the highest mean z-score of calcium signal exhibited the lowest freezing behavior, $P = 0.002$, $\eta^2 = 0.21$. (*I* and *J*) Timeseries of peak calcium signal. (*I*) Cumulative frequency distribution of proportion of peak calcium signal across the 20-s cue by condition. Dashed line is included as a depiction of evenly distributed signal. (*J*) Quantification of proportion of peak calcium signal by 5-s epochs. The threat condition showed a significantly greater proportion of peak calcium signal during 0 to 5 s than 6 to 10 s, 11 to 15 s, and 16 to 20 s (Tukey's HSD, Ps = 0.005, 0.030, and 0.013). The compound condition showed a significantly greater proportion of peak calcium signal during 0 to 5 s than 11 to 15 s (Tukey's HSD, $P = 0.009$). All error bars show ± 1 SEM. *$P < 0.05$, **$P < 0.01$, ***$P < 0.001$.

the duration of the safety cue presentations was evenly distributed (all *P*s >0.161). Together, these data indicate that PL-projecting ventral hippocampal neurons exhibit a strong response to the immediate presence of a threat while also emphasizing the importance of continuous neural activity for processing the safety information of a cue.

Consistent with the results for average calcium activity (Fig. 3*C*), the average magnitude of the peak calcium signal differed between threat, compound, and safety conditions, [$F(2, 39) = 6.13$, $P = 0.005$, $\eta^2 = 0.24$, driven by a linear increase across threat, compound, and safety cues, $F(1, 39) = 11.17$, $P = 0.002$, $\eta^2 = 0.22$ (*SI Appendix*, Fig. S4)]. These data suggest that safety and compound cues may elicit a higher magnitude of neural activity than threat cues, and also, that the relative absence of fluctuations in proportion of peak signal across the duration of the compound and safety cues reflects only the absence of temporal coordination of neural firing, rather than a reduction in neural activity altogether. Taken together, data obtained from PL-projecting ventral hippocampal neurons suggest that both the overall magnitude and the timeseries of neural activity may be key determinants in processing safety information and in inhibiting threat responding.

Analysis of the timeseries of peak calcium signal in cumulative ventral hippocampal neurons [main effect of epoch, $F(3, 105) = 17.67$, $P < 0.001$, $\eta_p^2 = 0.31$, and interaction between condition and epoch, $F(6, 105) = 2.40$, $P = 0.032$, $\eta_p^2 = 0.08$] and IL-projecting neurons [main effect of epoch, $F(3, 99) = 10.91$, $P < 0.001$, $\eta_p^2 = 0.21$, and interaction between condition and epoch, $F(6, 99) = 3.60$, $P = 0.003$, $\eta_p^2 = 0.14$] indicated a similar pattern of onset-locked responsiveness to threat cues; but in contrast to PL-projecting neurons, a greater proportion of peak calcium signal at tone onset was also observed for compound cues (*SI Appendix*, Figs. S2*A* and S6*A*). Thus, the onset of a threat cue, both alone and in compound with the safety cue, elicits a transient coordination of neuronal firing. Subsequently, the pattern of onset-locked responsiveness is maintained for both threat and compound conditions, although the precise distribution of proportion of peak calcium signal differed between the 2 conditions for both neuronal populations. Activity was continuously distributed during safety cues in both cumulative ventral hippocampal neurons and IL-projecting neurons. For BLA-projecting neurons, all 3 conditions exhibited a higher proportion of peak calcium signal associated with cue onset relative to all other epochs [main effect of epoch, $F(3, 81) = 17.26$, $P < 0.001$, $\eta^2 = 0.37$], although the timeseries of peak calcium signal did not differ between conditions [*SI Appendix*, Fig. S9*A*, no interaction effect, $F(6, 81) = 0.80$, $P = 0.570$, $\eta_p^2 = 0.03$]. Thus, BLA-projecting ventral hippocampal neurons may respond to the presence of a salient cue, but do not differentiate between the threat and safety properties of the cue.

The mean magnitude of peak calcium signal differed between threat, compound, and safety conditions for both cumulative [1-way ANOVA, $F(2, 35) = 3.88$, $P = 0.030$, $\eta^2 = 0.18$, linear increase across threat, compound, and safety cues, $F(1, 35) = 7.72$, $P = 0.009$, $\eta^2 = 0.18$] and IL-projecting ventral hippocampal neurons [1-way ANOVA, $F(2, 33) = 3.83$, $P = 0.032$, $\eta^2 = 0.19$, linear increase across threat, compound, and safety cues, $F(1, 33) = 6.71$, $P = 0.014$, $\eta^2 = 0.17$], with a marginal trend apparent in BLA-projecting neurons [1-way ANOVA, $F(2, 27) = 2.61$, $P = 0.092$, $\eta_p^2 = 0.16$]. While these data suggest an increased magnitude of calcium signaling, this increase was consistent with overall higher levels of neural activity only in cumulative ventral hippocampal neurons (Fig. 2*C*), but not IL- or BLA-projecting neurons (*SI Appendix*, Figs. S5*F* and S8*F*).

Discussion

Despite the substantial need for enhanced approaches to target fear reduction and inform interventions for anxiety based on the neurobiology of safety signal learning, the neural mechanisms of fear inhibition via safety signals have remained unclear. The present study investigated the neural substrates of conditioned inhibition across species. Collectively, our findings demonstrate parallel behavioral and neural activity patterns during conditioned inhibition in both mice and humans. In particular, we show evidence of hippocampal involvement, specifically related to ventral hippocampal–PL (ventral hippocampal–dACC in humans) (43) interactions, highlighting a specific pathway associated with threat inhibition by safety signals across species. These findings point toward the potential for using safety signals as a translational tool to target an alternative neural pathway and optimize current interventions for stress-related and anxiety disorders.

Our data build upon a growing literature highlighting a critical role of the ventral hippocampus in informing the degree of threat or safety in an environment (36, 46, 47) and suggest that the hippocampus may be involved in the active inhibition of threat responding via safety (i.e., the implementation of learned safety). Within the ventral hippocampus in mice, and the homologous anterior hippocampus in humans, neural activity was elevated during conditioned inhibition, relative to the threat cue alone. Furthermore, activation of the ventral hippocampus in mice was continuously higher throughout the latter half of compound cues and the entirety of safety cues, which was absent during threat cues. One possibility is that this continuous activity allows for recruitment of additional circuitry, such as the striatum (28), that facilitates a reduction in threat responding.

In humans, ventral hippocampal activation during the compound condition was highest, relative to the safety or threat cues alone, suggesting the potential for different mechanisms at play between the recall of a safety cue (i.e., explicit safety) versus conditioned inhibition. In mice, average activity was elevated in response to both the safety cue alone and the compound condition, relative to the threat cue. Thus, while activity in the ventral hippocampus in mice may be related to learned safety more generally, this region may play a more specific role in the conditioned inhibition of threat responding in humans.

The ventral hippocampus may engage in the complex regulation of threat responding by parcellating information about the presence of a stimulus, the valence or emotional significance of that stimulus, and the appropriate behavioral response, and by conveying distinct pieces of information to different brain regions. Notably, the PL-projecting subpopulation of ventral hippocampal neurons were the only neurons to show higher activity during both compound and safety cues relative to threat cues as well as a significant association between neural activity and freezing behavior. This finding highlights a novel role for PL-projecting ventral hippocampal neurons during the inhibition of threat responding in the presence of a safety signal. Previously, Sotres-Bayon et al. found that inactivating the ventral hippocampus after extinction disrupted fear inhibition, such that animals showed increased fear expression (47). This finding suggests that the ventral hippocampus inhibits fear expression after, but not before, extinction. The present findings suggest that the ventral hippocampus may play a similar role in inhibiting fear expression during conditioned inhibition. In this way our investigation extends the literature by considering the neural dynamics of the active inhibition of a threat response, where classic mechanisms for cued threat recall are attenuated or altered by the presence of a safety signal. Moreover, while ventral hippocampal projections to medial PFC have been shown to reduce anxiety-like phenotypes in anxiogenic environments (46), our data highlight a specific role of PL-projecting ventral hippocampal neurons for the conditioned inhibition of responding to discrete stimuli.

It is plausible that the ventral hippocampus mediates conditioned inhibition by producing a net inhibition of PL through contacts with inhibitory interneurons (47), thus reducing the capacity of PL to initiate an overt threat response (9, 38). Indeed, an additional finding of Sotres-Bayon et al. was that ventral hippocampal projections activated inhibitory interneurons in the

PL, suggesting there is feed-forward inhibition in this pathway (47). Furthermore, inactivation of the ventral hippocampus increased PL tone responsiveness, suggesting that the ventral hippocampus may be gating conditioned responses in the PL (47). This result is congruent with our present findings in which lower fear expression in conditioned inhibition was inversely related to ventral hippocampal activity, but only in neurons projecting to the PL.

Paralleling the findings in PL-projecting ventral hippocampal neurons in mice, evidence in humans highlighted the involvement of interactions between the ventral hippocampus and the dACC in conditioned inhibition. The strong negative correlation between activity in the hippocampus and dACC that was observed during presentations of a threat cue may suggest that these regions are "out of sync" when threat is imminent. Indeed, previous research has found that anterior cingulate projections to the hippocampus may underlie top-down prefrontal gating of contextual memory retrieval (48). As such, asynchronous activity between the dACC and ventral hippocampus could support top-down control of hippocampal activity in response to imminent threat, but not safety. The lack of differential hippocampal–anterior vmPFC (IL homolog; ref. 44) or hippocampal–BLA functional connectivity between threat, compound, and safety conditions further parallels the observed results in mice, highlighting the potential specificity of PL/dACC involvement in conditioned inhibition and pointing to the importance of this specific circuit for threat regulation across species.

While previous research has used inactivation methods in the rodent brain to investigate the circuitry mediating conditioned inhibition, here we examined the temporal dynamics of neural activity during the active inhibition of threat responding. A transient increase in neural activity (i.e., a higher proportion of peak calcium signal) was apparent immediately following the onset of a threat cue, but never a safety cue (with the possible exception of BLA-projecting neurons in which no condition-specific responses were observed). Thus, an intriguing possibility is that peak activity induced via tone onset reflects a "startle response" that initiates a calculation of the "fear properties" of the tone. In line with this idea, we have previously shown a similar increase in neural activity in PL-projecting ventral hippocampal neurons time-locked to the onset of a threat cue following Pavlovian fear conditioning (49). This initial activity in ventral hippocampus may serve to prime additional circuitry to respond to a potential threat. Subsequently, the persistence of neural activity during compound cues, apparent only in PL-projecting neurons and contrasting with a rapid and continued attenuation of activity during threat cues, may override or modify the circuitry primed for threat responding.

Interestingly, the proportion of peak calcium signal in response to the onset of a compound cue was greatest in IL-projecting ventral hippocampal neurons, with more peak signal occurring within the first 5 s relative to any other time in the cue. This pattern could indicate a role for this circuit in processing the ambiguity of the compound cue, information that may then be relayed to additional circuits (e.g., IL-mediated inhibition of BLA) to attenuate threat responding during the compound condition (e.g., ref. 20). Finally, BLA-projecting neurons appear to respond indiscriminately to the presence of salient stimuli. These data are consistent with evidence that BLA-projecting ventral hippocampal neurons encode valence-related contextual information, but are not involved in mediating avoidance behavior in an anxiogenic context (34). In addition, while previous research has shown an increase in synchronous activity between the ventral hippocampus and the BLA specifically during a threat cue, but not a neutral cue (50), our research extends this by showing that BLA-projecting ventral hippocampal neurons may also play a role in processing safety information. Pharmacological and lesion studies disrupting ventral hippocampal activity following conditioning, but not following extinction, have reported reduced expression of threat responding (38, 39, 47). However, such methods disrupt signaling throughout the duration of a behavioral session, and lesions may lead to compensatory changes that complicate the interpretation of these results. Our data indicate that dynamic fluctuations in neural activity during specific periods of the cue presentation (e.g., tone onset vs. late tone) may be critical for modulating fear or safety behaviors. Whereas rapid immediate processing may reflect the initial response to the "threat properties" of a stimulus, the more protracted neural dynamics across the duration of the stimulus (e.g., circuit engagement) may critically determine adjustments in the representational value of the stimulus as well as overall levels of threat responding. Given these differences in the neural dynamics across conditions, future studies should focus on methods to inactivate these hippocampal projection neurons to test the causal involvement of the ventral hippocampus in conditioned inhibition.

Although the use of parallel conditioned inhibition tasks across species is a major strength of the present study, several limitations should be addressed in future research. In humans, only a subsample of participants ($n = 22$) could be included in the SCR analysis due to low overall SCR signal ($n = 12$), lack of sustained learning ($n = 17$; defined as a positive nonzero difference in SCR to threat versus safety cues during the first half of the testing phase), and technical problems ($n = 3$). The observation of low overall signal in a subsample of participants is a common problem in human studies that rely on SCR (51), and future studies would benefit from a larger sample that accounts for the loss of data due to nonresponders and nonlearners. Furthermore, although the testing phase of the conditioned inhibition task in humans included a novel compound, this condition was not included in the parallel task in mice. Future studies would benefit from including this condition in both rodents and humans to control for the novelty of presenting a compound stimulus during conditioned inhibition. Other task differences between mouse and human paradigms existed, including different cue modalities, unconditioned stimulus (US) modalities, task timing (i.e., across multiple days versus across a single scan session), and output measurements (i.e., freezing behavior vs. skin conductance). Many of these differences were necessary given species-specific behavior. For example, to date, there are inconsistent findings on rodent shape processing and visual acuity (52), which made the auditory modality more appropriate for the task paradigm in rodents. Though these task differences are consistent with prior cross-species studies (e.g., ref. 53; for a review, see ref. 54) and the present findings suggest similar underlying processes, future studies may benefit from using more similar task designs across species.

Testing the efficacy of safety signals and identifying the neural mechanisms by which they reduce fear are critical for informing whether and how the integration of safety signals could augment interventions for anxiety disorders. The primary evidence-based psychosocial treatment for individuals with anxiety and stress-related disorders is exposure-based CBT, which is based on principles of fear extinction (1, 4, 14). During exposure-based therapy, patients repeatedly and systematically confront fear-provoking stimuli with the goal to reduce anxiety (55, 56). However, fear extinction is weaker among individuals with anxiety (9, 10), and up to 50% of individuals with anxiety disorders do not respond sufficiently to CBT (4, 5). Additionally, up to 27% of patients drop out of treatment (57), possibly due to the aversive nature of the exposures themselves (55). These findings suggest that patients with anxiety disorders may benefit from other methods of fear reduction, particularly the incorporation of safety signals to enhance efficacy and tolerability.

By using conditioned inhibition to leverage an alternative neural circuit, our findings have the potential to optimize treatment for anxiety disorders. Here we show that safety signals engage the ventral hippocampus during the inhibition of threat responding. Moreover, our results highlight the specific engagement

of a subpopulation of these neurons projecting to the PL in mice, and homologous ventral hippocampal–dACC connectivity in humans. This pathway for inhibiting threat responding diverges from the circuitry involved in extinction learning, which has largely implicated the IL, and homologous anterior vmPFC in humans, for the suppression of fear (14, 37). Notably, patients with anxiety disorders do not recruit the vmPFC to the same extent as healthy controls during fear inhibition (58) and display weaker structural and functional vmPFC–amygdala connectivity that results in limited top-down control of amygdala reactivity (11). Thus, targeting a distinct pathway via safety signals may provide an effective alternative or means to enhance treatment for individuals for whom the efficacy of exposure-based CBT is otherwise limited.

Methods

Mice. Male mice (C57BL/6J, The Jackson Laboratory) were group housed in cages of 3 to 5 and randomly allocated to experimental groups. All mice were healthy with no obvious behavioral phenotypes. Experiments were carried out in accordance with the National Institutes of Health's Guide for the Care and Use of Laboratory Animals, and protocols were approved by the Weill Medical College of Cornell University's Institutional Animal Care and Use Committee. Details are provided in *SI Appendix*.

Surgical Procedures. Separate groups of mice were anesthetized with a ketamine and xylazine mixture (100 mg/mL and 10 mg/mL, respectively) and unilaterally injected with AAV1-Syn-GCaMP6s (Addgene Plasmid Repository) to provide a measure of cumulative ventral hippocampal activity, or a Cre-recombinase activated strain of the GCaMP virus (AAV5-Syn-FLEX-GCaMP6s, Addgene Plasmid Repository) in the ventral hippocampus and a retrograde Cre-recombinase (rAAV2-retro/CAG-Cre, the Vector Core at the University of North Carolina at Chapel Hill) used to isolate GCaMP expression to subpopulations of interest. The retro-Cre virus was infused into either PL, IL, or BLA. At each site GCaMP (200 nL) or retro-Cre (150 nL) viral constructs were infused at a rate of 50 nL/min using a NanoFil syringe connected to an infusion pump. All coordinates were based on ref. 59 and values were relative to bregma (anterior/posterior, AP; medial/lateral, ML) and brain surface (dorsal/ventral, DV). Ventral hippocampus: AP3.2, ML3.1, and DV3.2 mm; PL: AP2.2, ML0.3, and DV1.35 mm; IL: AP1.65, ML0.3, and DV2.2 mm; and BLA: AP1.5, ML3.0, and DV3.65 mm. A mono fiber-optic cannula (Doric Lenses) with a 0.48-refractive index and a 400-nm diameter was implanted into the ventral hippocampus ~0.05 mm above the viral injection depth and fixed to the skull using Metabond Quick Adhesive Cement. Recovery and expression of the transgenes was allowed to take place over the course of 4 wk before the beginning of behavioral training. Details are provided in *SI Appendix*.

Animal Behavior. Behavioral procedures were carried out in standard conditioning chambers (Med Associates) enclosed in a cubicle containing a surveillance camera used to monitor the mice during behavioral training. During the training phase, for 4 consecutive days, all mice were trained to discriminate between threat and safety cues (a 2.9-kHz tone or a 12.5-kHz tone, both 80 dB, played for 20 s and counterbalanced as threat or safety). Presentations of the threat cue coterminated with a mild footshock (0.5 mA, 1-s duration). Mice were exposed to 2 presentations of the threat cue and 30 presentations of the safety cue each day, with the trial order varied daily. On day 5, the testing phase, mice were connected to a patch cord allowing for live recording of calcium signaling. Behavioral testing and fiber photometry recording took place in a novel conditioning chamber (differentiated by visual, tactile, and olfactory features) in order to isolate cue-elicited behavioral responding from residual contextual fear. Separate groups of mice were exposed to 10 20-s presentations of a threat, safety, or compound cue in the absence of shock. For behavioral analysis, the percentage of time spent freezing during the tone was averaged across the 10 trials for each condition (threat, compound, and safety) and subjected to a 1-way ANOVA followed by a linear contrast for between-group analysis. Each hypothesis was tested at a level of significance $\alpha = 0.05$. Details are provided in *SI Appendix*.

Fiber Photometry. Four weeks following recovery from surgery, mice underwent conditioned inhibition training (i.e., acquisition phase; days 1 to 4; Fig. 1 *A*, *Top*), and GCaMP signal was recorded during the testing phase (day 5; Fig. 1 *A*, *Bottom*). The fiber photometry rig was based on a design described in detail elsewhere (45, 60) and fiber photometry protocols were carried out as described in ref. 49. Light from a 470-nm LED (Thorlabs) served to excite neurons such that those neurons expressing the GCaMP emitted an activity-dependent fluorescent signal (44, 58). Fiber photometry data were analyzed in MATLAB (MathWorks). Fluorescent signal was normalized to the median [$\Delta F/F$; as described in ref. 49 and *SI Appendix*] and transformed to a z-score to allow comparison of calcium signal magnitude between mice. Data were analyzed for individual trials based on a pulse from the behavioral system (Video Freeze Software) that interfaced with the fiber photometry console and allowed fluorescent signal to be time-locked to stimulus presentations. Details on the fiber photometry equipment, and preprocessing and analyses of fiber photometry data are provided in *SI Appendix*.

Histology. Mice were anesthetized with an overdose of sodium pentobarbital and transcardially perfused with 0.9% saline followed by 4% paraformaldehyde in 0.01 M sodium phosphate buffer (PB) (pH 7.4). The brains were then removed and postfixed with 4% paraformaldehyde in 0.01 M sodium phosphate buffer at 4 °C overnight and transferred to a sucrose solution (30% sucrose in 0.1 M PB) at 4 °C for 48 h. Coronal sections (40 μm) were analyzed to verify expression of the GCaMP virus and placement of the optical fiber. Mice with inaccurate targeting were eliminated from the study. Details are provided in *SI Appendix*.

Human Participants. Participants were 54 healthy adults between the ages of 18 and 30. All participants were free of current or past psychiatric disorders, psychotropic medication-naïve, right-handed, and had an IQ of at least 80. Study procedures were approved by the institutional review board at Yale University, and all participants provided written informed consent. Details are provided in *SI Appendix*.

Conditioned Inhibition Task in Humans. During fMRI data collection, participants completed a conditioned inhibition task (Fig. 1*B*). This task was adapted from the AX+/BX– task of conditioned inhibition (16, 18) to be used during fMRI collection and specifically with children and adolescents in related studies. Conditioned stimuli (CS) were neutral geometric shapes of different colors; the US was an aversive metallic noise (61) delivered at 95 to 100 dBC through MRI-safe noise-cancelling headphones (www.optoacoustics.com). Details are provided in *SI Appendix*.

Analysis of Physiological Data in Humans. To measure physiological responses associated with fear during the conditioned inhibition task, we assessed SCR using a Biopac MRI-compatible skin conductance recording system (https://www.biopac.com/) together with AcqKnowledge software (https://www.biopac.com/product/acqknowledge-software/) to amplify and record the SCR. Details on quality assurance, preprocessing, and analyses of physiological data are provided in *SI Appendix*.

Analysis of MRI Data in Humans.

MRI acquisition parameters. Participants were scanned on a 3T Siemens Magnetom Prisma scanner using a 32-channel head coil. A whole-brain high-resolution T1-weighted anatomical scan magnetization-prepared rapid acquisition gradient echo (MPRAGE) was collected, as well as high spatial and temporal resolution multiband echo planar imaging (EPI) fMRI scans during the conditioned inhibition task. Details are provided in *SI Appendix*.

fMRI preprocessing. Raw neuroimaging data were converted to Brain Imaging Data Structure (BIDS; ref. 62) using heudiconv (https://github.com/nipy/heudiconv) and preprocessed with the Human Connectome Project (HCP) minimal preprocessing pipeline (63) using the HCP Pipelines BIDS app (https://github.com/BIDS-Apps/HCPPipelines) version 3.17.14. Details are provided in *SI Appendix*.

fMRI individual-level analysis. fMRI data analyses were carried out using FEAT (FMRI Expert Analysis Tool) version 6.00, part of Functional Magnetic Resonance Imaging of the Brain (FMRIB) Software Library (FSL, https://fsl.fmrib.ox.ac.uk/fsl/fslwiki) version 5.0.10 with FILM autocorrelation correction (64). Rigorous motion correction was implemented to limit the potential effects of motion on task-related results. Standard and extended motion parameters output from FSL's MCFLIRT (65) during HCP minimal preprocessing were added as nuisance regressors in each participant's lower-level design matrices. Additionally, FSL's fsl_motion_outliers function was used to detect timepoints that were corrupted by large motion in each participant's data. Details are provided in *SI Appendix*.

Activation analysis. Based on a priori hypotheses regarding the involvement of the ventral hippocampus in conditioned inhibition, we conducted a ROI analysis using FSL's featquery tool to extract mean percent signal change for each condition (threat, safety, and safety compound) during the testing phase of the conditioned inhibition task following each subject's individual-level analysis. Right and left anterior hippocampal masks were obtained from ref. 66 in which the full hippocampus was defined probabilistically based on an in-house

database of manual segmentations, which were then divided into anterior and posterior subregions by drawing a plane at y = −21. This ROI is referred to as the ventral hippocampus. Each hypothesis was tested at a level of significance $\alpha = 0.05$. Additional details are provided in *SI Appendix*.

Functional connectivity analysis. A gPPI analysis was conducted using FEAT version 6.00, part of FSL (https://fsl.fmrib.ox.ac.uk/fsl/fslwiki) version 5.0.10 with FILM autocorrelation correction (64). The gPPI analysis allowed for an examination of task-evoked functional connectivity of the ventral hippocampus with the dACC and with the anterior vmPFC, which are thought to correspond to PL and IL in rodents, respectively (43, 44), and with the BLA. Details are provided in *SI Appendix*.

Data Availability. Data used for these studies have been deposited in the Open Science Framework Repository (67) (https://osf.io/nqryd/?view_only=dbcea56e594c41a1b741da18db70d6bd).

ACKNOWLEDGMENTS. This work was supported by the NIH Director's Early Independence Award (DP5OD021370) to D.G.G., Brain & Behavior Research Foundation (National Alliance for Research on Schizophrenia and Depression) Young Investigator Award to D.G.G., Jacobs Foundation Early Career Research Fellowship to D.G.G., NIH R01 (NS052819) to F.S.L., Pritzker Neuropsychiatric Disorders Research Consortium Award to F.S.L., the New York Presbyterian Youth Anxiety Center (F.S.L.), the Dr. Mortimer D. Sackler family (F.S.L.), the DeWitt-Wallace Fund of the New York Community Trust (F.S.L. and H.C.M.), NIH K99MH119320 National Institute of Mental Health Pathway to Independence Award (to H.C.M.), the National Center for Advancing Translational Science of the NIH TL1 Award (TR0002386) to H.C.M., and National Science Foundation Graduate Research Fellowship Program Award (DGE1122492) to P.O. We gratefully acknowledge Camila Caballero, Emma Goodman, Cristian Hernandez, Sahana Kribakaran, Sarah McCauley, Luise Pruessner, and Hopewell Rogers for assistance with data collection and BJ Casey and Nim Tottenham for generous support and feedback during study conceptualization and design.

1. B. O. Rothbaum, M. Davis, Applying learning principles to the treatment of post-trauma reactions. *Ann. N. Y. Acad. Sci.* **1008**, 112–121 (2003).
2. R. C. Kessler *et al*., Prevalence and treatment of mental disorders, 1990 to 2003. *N. Engl. J. Med.* **352**, 2515–2523 (2005).
3. T. Vos *et al*.; GBD 2015 Disease and Injury Incidence and Prevalence Collaborators, Global, regional, and national incidence, prevalence, and years lived with disability for 310 diseases and injuries, 1990-2015: A systematic analysis for the Global Burden of Disease Study 2015. *Lancet* **388**, 1545–1602 (2016).
4. A. N. Kaczkurkin, E. B. Foa, Cognitive-behavioral therapy for anxiety disorders: An update on the empirical evidence. *Dialogues Clin. Neurosci.* **17**, 337–346 (2015).
5. A. G. Loerinc *et al*., Response rates for CBT for anxiety disorders: Need for standardized criteria. *Clin. Psychol. Rev.* **42**, 72–82 (2015).
6. J. P. Johansen, C. K. Cain, L. E. Ostroff, J. E. LeDoux, Molecular mechanisms of fear learning and memory. *Cell* **147**, 509–524 (2011).
7. S. Maren, Neurobiology of Pavlovian fear conditioning. *Annu. Rev. Neurosci.* **24**, 897–931 (2001).
8. M. E. Bouton, Context, ambiguity, and unlearning: Sources of relapse after behavioral extinction. *Biol. Psychiatry* **52**, 976–986 (2002).
9. K. A. Corcoran, G. J. Quirk, Recalling safety: Cooperative functions of the ventromedial prefrontal cortex and the hippocampus in extinction. *CNS Spectr.* **12**, 200–206 (2007).
10. J. Haaker *et al*., Deficient inhibitory processing in trait anxiety: Evidence from context-dependent fear learning, extinction recall and renewal. *Biol. Psychol.* **111**, 65–72 (2015).
11. M. J. Kim *et al*., The structural and functional connectivity of the amygdala: From normal emotion to pathological anxiety. *Behav. Brain Res.* **223**, 403–410 (2011).
12. D. C. Johnson, B. J. Casey, Easy to remember, difficult to forget: The development of fear regulation. *Dev. Cogn. Neurosci.* **11**, 42–55 (2015).
13. E. A. Phelps, M. R. Delgado, K. I. Nearing, J. E. LeDoux, Extinction learning in humans: Role of the amygdala and vmPFC. *Neuron* **43**, 897–905 (2004).
14. M. R. Milad, G. J. Quirk, Fear extinction as a model for translational neuroscience: Ten years of progress. *Annu. Rev. Psychol.* **63**, 129–151 (2012).
15. J. P. Christianson *et al*., Inhibition of fear by learned safety signals: A mini-symposium review. *J. Neurosci.* **32**, 14118–14124 (2012).
16. K. M. Myers, M. Davis, AX+, BX- discrimination learning in the fear-potentiated startle paradigm: Possible relevance to inhibitory fear learning in extinction. *Learn. Mem.* **11**, 464–475 (2004).
17. A. M. Kazama, K. B. Schauder, M. McKinnon, J. Bachevalier, M. Davis, A novel AX+/BX- paradigm to assess fear learning and safety-signal processing with repeated-measure designs. *J. Neurosci. Methods* **214**, 177–183 (2013).
18. T. Jovanovic *et al*., Fear potentiation and fear inhibition in a human fear-potentiated startle paradigm. *Biol. Psychiatry* **57**, 1559–1564 (2005).
19. A. R. Foilb, J. P. Christianson, "11–Brain mechanisms for learning and using safety signals" in *Neurobiology of Abnormal Emotion and Motivated Behaviors*, S. Sangha, D. Foti, Eds. (Academic Press, 2018), pp. 204–222.
20. E. Kong, F. J. Monje, J. Hirsch, D. D. Pollak, Learning not to fear: Neural correlates of learned safety. *Neuropsychopharmacology* **39**, 515–527 (2014).
21. S. Sangha, P. D. Robinson, Q. Greba, D. A. Davies, J. G. Howland, Alterations in reward, fear and safety cue discrimination after inactivation of the rat prelimbic and infralimbic cortices. *Neuropsychopharmacology* **39**, 2405–2413 (2014).
22. M. C. Sarlitto, A. R. Foilb, J. P. Christianson, Inactivation of the ventrolateral orbitofrontal cortex impairs flexible use of safety signals. *Neuroscience* **379**, 350–358 (2018).
23. A. R. Foilb, J. G. Flyer-Adams, S. F. Maier, J. P. Christianson, Posterior insular cortex is necessary for conditioned inhibition of fear. *Neurobiol. Learn. Mem.* **134**, 317–327 (2016).
24. R. Genud-Gabai, O. Klavir, R. Paz, Safety signals in the primate amygdala. *J. Neurosci.* **33**, 17986–17994 (2013).
25. A. M. Kazama, E. Heuer, M. Davis, J. Bachevalier, Effects of neonatal amygdala lesions on fear learning, conditioned inhibition, and extinction in adult macaques. *Behav. Neurosci.* **126**, 392–403 (2012).
26. K. H. Ng, M. W. Pollock, P. J. Urbanczyk, S. Sangha, Altering D1 receptor activity in the basolateral amygdala impairs fear suppression during a safety cue. *Neurobiol. Learn. Mem.* **147**, 26–34 (2018).
27. L. E. Ostroff, C. K. Cain, J. Bedont, M. H. Monfils, J. E. Ledoux, Fear and safety learning differentially affect synapse size and dendritic translation in the lateral amygdala. *Proc. Natl. Acad. Sci. U.S.A.* **107**, 9418–9423 (2010).
28. M. T. Rogan, K. S. Leon, D. L. Perez, E. R. Kandel, Distinct neural signatures for safety and danger in the amygdala and striatum of the mouse. *Neuron* **46**, 309–320 (2005).
29. E. Likhtik, J. M. Stujenske, M. A. Topiwala, A. Z. Harris, J. A. Gordon, Prefrontal entrainment of amygdala activity signals safety in learned fear and innate anxiety. *Nat. Neurosci.* **17**, 106–113 (2014).
30. J. P. Christianson *et al*., Safety signals mitigate the consequences of uncontrollable stress via a circuit involving the sensory insular cortex and bed nucleus of the stria terminalis. *Biol. Psychiatry* **70**, 458–464 (2011).
31. J. P. Christianson *et al*., The sensory insular cortex mediates the stress-buffering effects of safety signals but not behavioral control. *J. Neurosci.* **28**, 13703–13711 (2008).
32. N. M. Fournier, R. S. Duman, Illuminating hippocampal control of fear memory and anxiety. *Neuron* **77**, 803–806 (2013).
33. J. E. LeDoux, Emotion circuits in the brain. *Annu. Rev. Neurosci.* **23**, 155–184 (2000).
34. J. C. Jimenez *et al*., Anxiety cells in a hippocampal-hypothalamic circuit. *Neuron* **97**, 670–683.e6 (2018).
35. Q. Wang, J. Jin, S. Maren, Renewal of extinguished fear activates ventral hippocampal neurons projecting to the prelimbic and infralimbic cortices in rats. *Neurobiol. Learn. Mem.* **134**, 38–43 (2016).
36. J. Ji, S. Maren, Hippocampal involvement in contextual modulation of fear extinction. *Hippocampus* **17**, 749–758 (2007).
37. J. A. Hobin, J. Ji, S. Maren, Ventral hippocampal muscimol disrupts context-specific fear memory retrieval after extinction in rats. *Hippocampus* **16**, 174–182 (2006).
38. D. Sierra-Mercado, N. Padilla-Coreano, G. J. Quirk, Dissociable roles of prelimbic and infralimbic cortices, ventral hippocampus, and basolateral amygdala in the expression and extinction of conditioned fear. *Neuropsychopharmacology* **36**, 529–538 (2011).
39. S. Maren, W. G. Holt, Hippocampus and Pavlovian fear conditioning in rats: Muscimol infusions into the ventral, but not dorsal, hippocampus impair the acquisition of conditional freezing to an auditory conditional stimulus. *Behav. Neurosci.* **118**, 97–110 (2004).
40. V. M. Chen, A. R. Foilb, J. P. Christianson, Inactivation of ventral hippocampus interfered with cued-fear acquisition but did not influence later recall or discrimination. *Behav. Brain Res.* **296**, 249–253 (2016).
41. S. A. Heldt, G. D. Coover, W. A. Falls, Posttraining but not pretraining lesions of the hippocampus interfere with feature-negative discrimination of fear-potentiated startle. *Hippocampus* **12**, 774–786 (2002).
42. R. J. McDonald *et al*., Rats with ventral hippocampal damage are impaired at various forms of learning including conditioned inhibition, spatial navigation, and discriminative fear conditioning to similar contexts. *Behav. Brain Res.* **351**, 138–151 (2018).
43. M. R. Milad *et al*., A role for the human dorsal anterior cingulate cortex in fear expression. *Biol. Psychiatry* **62**, 1191–1194 (2007).
44. M. R. Milad *et al*., Recall of fear extinction in humans activates the ventromedial prefrontal cortex and hippocampus in concert. *Biol. Psychiatry* **62**, 446–454 (2007).
45. L. A. Gunaydin *et al*., Natural neural projection dynamics underlying social behavior. *Cell* **157**, 1535–1551 (2014).
46. N. Padilla-Coreano *et al*., Direct ventral hippocampal-prefrontal input is required for anxiety-related neural activity and behavior. *Neuron* **89**, 857–866 (2016).
47. F. Sotres-Bayon, D. Sierra-Mercado, E. Pardilla-Delgado, G. J. Quirk, Gating of fear in prelimbic cortex by hippocampal and amygdala inputs. *Neuron* **76**, 804–812 (2012).
48. P. Rajasethupathy *et al*., Projections from neocortex mediate top-down control of memory retrieval. *Nature* **526**, 653–659 (2015).
49. J. I. Giza *et al*., The BDNF Val66Met prodomain disassembles dendritic spines altering fear extinction circuitry and behavior. *Neuron* **99**, 163–178.e6 (2018).
50. T. Seidenbecher, T. R. Laxmi, O. Stork, H.-C. Pape, Amygdalar and hippocampal theta rhythm synchronization during fear memory retrieval. *Science* **301**, 846–850 (2003).
51. T. B. Lonsdorf *et al*., Don't fear 'fear conditioning': Methodological considerations for the design and analysis of studies on human fear acquisition, extinction, and return of fear. *Neurosci. Biobehav. Rev.* **77**, 247–285 (2017).
52. V. Djurdjevic, A. Ansuini, D. Bertolini, J. H. Macke, D. Zoccolan, Accuracy of rats in discriminating visual objects is explained by the complexity of their perceptual strategy. *Curr. Biol.* **28**, 1005–1015.e5 (2018).
53. S. S. Pattwell *et al*., Altered fear learning across development in both mouse and human. *Proc. Natl. Acad. Sci. U.S.A.* **109**, 16318–16323 (2012).

54. J. Haaker, *et al*., Making translation work: Harmonizing cross-species methodology in the behavioural neuroscience of Pavlovian fear conditioning. *Neurosci. Biobehav. Rev.* **107**, 329–345 (2019).
55. P. J. Norton, E. C. Price, A meta-analytic review of adult cognitive-behavioral treatment outcome across the anxiety disorders. *J. Nerv. Ment. Dis.* **195**, 521–531 (2007).
56. M. G. Craske, M. Treanor, C. C. Conway, T. Zbozinek, B. Vervliet, Maximizing exposure therapy: An inhibitory learning approach. *Behav. Res. Ther.* **58**, 10–23 (2014).
57. E. Hans, W. Hiller, A meta-analysis of nonrandomized effectiveness studies on outpatient cognitive behavioral therapy for adult anxiety disorders. *Clin. Psychol. Rev.* **33**, 954–964 (2013).
58. T. Greenberg, J. M. Carlson, J. Cha, G. Hajcak, L. R. Mujica-Parodi, Ventromedial prefrontal cortex reactivity is altered in generalized anxiety disorder during fear generalization. *Depress. Anxiety* **30**, 242–250 (2013).
59. G. Paxinos, K. B. J. Franklin, *Paxinos and Franklin's the Mouse Brain in Stereotaxic Coordinates* (Academic Press, Amsterdam, ed. 4, 2013).
60. G. Cui *et al*., Deep brain optical measurements of cell type-specific neural activity in behaving mice. *Nat. Protoc.* **9**, 1213–1228 (2014).
61. D. L. Neumann, A. M. Waters, H. R. Westbury, The use of an unpleasant sound as the unconditional stimulus in aversive Pavlovian conditioning experiments that involve children and adolescent participants. *Behav. Res. Methods* **40**, 622–625 (2008).
62. K. J. Gorgolewski *et al*., The brain imaging data structure, a format for organizing and describing outputs of neuroimaging experiments. *Sci. Data* **3**, 160044 (2016).
63. M. F. Glasser *et al*.; WU-Minn HCP Consortium, The minimal preprocessing pipelines for the Human Connectome Project. *Neuroimage* **80**, 105–124 (2013).
64. M. W. Woolrich, B. D. Ripley, M. Brady, S. M. Smith, Temporal autocorrelation in univariate linear modeling of FMRI data. *Neuroimage* **14**, 1370–1386 (2001).
65. M. Jenkinson, P. Bannister, M. Brady, S. Smith, Improved optimization for the robust and accurate linear registration and motion correction of brain images. *Neuroimage* **17**, 825–841 (2002).
66. N. C. Hindy, N. B. Turk-Browne, Action-based learning of multistate objects in the medial temporal lobe. *Cereb. Cortex* **26**, 1853–1865 (2016).
67. H. C. Meyer, P. Odriozola, F. S. Lee, D. G. Gee, Ventral hippocampus interacts with prelimbic cortex during inhibition of threat response via learned safety in both mice and humans. Open Science Framework. https://osf.io/nqryd/. Deposited 2 October 2019.
68. A. J. Shackman *et al*., The integration of negative affect, pain, and cognitive control in the cingulate cortex. *Nat. Rev. Neurosci.* **12**, 154–167 (2011).